

Received June 7, 2018, accepted July 12, 2018, date of publication July 23, 2018, date of current version August 15, 2018.

Digital Object Identifier 10.1109/ACCESS.2018.2858860

# Quantitative Resilience Assessment for Power Transmission Systems Under Typhoon Weather

YIHAO YANG, WENHU TANG<sup>D</sup>, (Senior Member, IEEE), YANG LIU,YANLI XIN, AND QINGHUA WU<sup>D</sup>, (Fellow, IEEE)

School of Electric Power Engineering, South China University of Technology, Guangzhou 510640, China

Corresponding author: Wenhua Tang (wenhutang@scut.edu.cn)

This work was supported in part by the National Natural Science Foundation of China under Grant 51477054 and in part by the China Postdoctoral Science Foundation under Grant 2017M620373.

**ABSTRACT** Reliable power grids are also vulnerable to extreme events, which are with a low probability but highly risk events, such as a typhoon. Power system, as an important infrastructure, should have the ability to withstand the adverse effect of such extreme events. This paper proposes a quantitative resilience assessment framework for power transmission systems operated under typhoon weather, which considers both the spatial and temporal impacts of typhoon. The proposed framework allows systematic estimation of resilience considering weather intensity, fault location of components, restoration resources, and emergency response plans. The typhoon wind field model for disaster risk assessment is applied to evaluate the intensity and the duration of impacts. The finite element modeling of components is developed to model the outage probability of components. A new resilience index considering the duration of extreme events (RICD) is proposed, which not only considers the performance of system but also considers characteristics of disruption. The proposed method is demonstrated by four case studies using the modified IEEE 6-bus test system. The numerical results reveal that the proposed method is able to quantify the influence of extreme event on power system resilience, and it shows that RICD is more feasible than two traditional indices in terms of normalization and comparability.

**INDEX TERMS** Extreme event, power transmission system, resilience assessment, sequential Monte Carlo simulation, typhoon.

## NOMENCLATURE

$A$	Index of areas.	$P_k$	Occurrence probability of fault scenario $k$ .
$B$	Pressure profile constant.	$P_1$	Overall breakdown probability of a transmission line.
$F$	Friction force of the atmospheric boundary layer.	$P_t$	Failure probability of all the towers in a corridor.
$f$	Coriolis force coefficient	$P_{li}$	Breakdown probability of segment $i$ .
$G$	Location of a power transmission system.	$P_{lj}$	Breakdown probability of tower $j$ .
$i$	Number of segments.	$p$	Mean sea level pressure.
$j$	Number of towers.	$p_0$	Central (minimum) pressure.
$K$	Total number of fault scenario occurrences.	$R$	Radial distance from typhoon center.
$k$	Fault scenario occurrences.	$R_a, R_b$	Radius of the last closed isobar.
$k_w$	Weather impact factors.	$R_m$	Radius of maximum wind speed.
$N_t$	Total number of segments in a transmission line.	$R_s$	Structural resistance.
$O$	Locations of typhoon centre.	$\bar{R}_s$	Mean value of structural resistance.
$P$	Failure probability	$S_{s,d}$	Structural stress or displacement.
$P_c$	Breakdown probability of a corridor.	$R_t, R_r, R_{RICD}$	Resilience metrics.
		$r$	Random number.
		$S$	Index of power system status.

$s$	Distance between the departure location of a repair team and a failure component.
$T$	Index of moments.
$t$	Simulation time.
$t_{\text{dur}}$	Duration of impact of typhoon.
$TTR$	Mean time to repair.
$V$	Typhoon-induced wind velocity.
$V_g$	Gradient wind.
$V'$	Wind caused by the friction on the ground surface.
$v$	Wind speed.
$v_r$	Average moving speed of a repair team.
$y$	Fitting parameter
$\Delta p$	Air pressure difference between the periphery and the center.
$\Delta t$	Simulation step.
$\Delta A$	Variations of $A$ .
$\beta$	Standard deviation.
$\rho$	Air density.
$\Phi(\cdot)$	Standard normal cumulative distribution function.
$E(\cdot)$	Expectation function.

## I. INTRODUCTION

The conventional power system planning schemes focus on reliability issues [1], which mainly investigate high-probability, low-impact events. Power system reliability evaluations usually assess the adequacy and security of power grids [2], [3]. In recent years, extreme disaster events caused several large-area power outages, which led to catastrophic impacts on daily activities of power customers, such as the icing disaster happened in 2008 in Southern China [4], the earthquake of Fukushima in Japan [5], and the terrorist attack at Metcalf substation in California [6]. These events highlight the vulnerability of power systems facing catastrophic events. Therefore, the methodology for assessing system evaluating resilience should be developed to evaluate the impacts of high-impact, low-probability events on power systems.

Generally, resilience is used to evaluate the ability of a system to withstand disturbances and recover after disturbances, which is defined in different disciplines [7]–[9]. Within this context, the resilience of power system is referred to as the ability of a power system to anticipate, absorb, resist, respond to and rapidly recover from a disruption, caused by a high-impact, low-probability event [10]–[12]. Although the concepts of reliability and resilience are particularly similar, resilience encompasses reliability and there still exists variations including the objectives, the approaches, and the methods used for evaluation [13]. Practical solutions can be derived based on resilience assessment to deal with potential power system disruptions facing extreme events.

To support resilience evaluation of typhoon impacts on transmission systems, various wind field models (e.g., Shapiro [14], CE [15], Y. Meng *et al.* [16]) were built for modelling a typhoon wind field. Various models

attempted to describe power system responses after faults, such as the DC model based on OPA [17], the AC power flow model [18], the complex network model [19], and the stochastic model [20]. One key feature of power system resilience is to assess how a power system recovers. Different approaches were used for modeling the repair time during extreme weather events. [21] and [22] assumed that no repair takes place during the period of an extreme weather. The time to repair ( $TTR$ ) of power system components under adverse weather was determined to be in proportional to the weather intensity by a weighting factor in [23].  $TTR$  of component, which was modeled in the majority of current literatures, neglected the location of fault, the size of repair crew, and the emergency response plan.

Various methodologies and indices were developed recently for evaluating power grid resilience. 1) Regarding assessment methodologies, [24] reviewed practices for assessing power system resilience and presented a load restoration method to assess resilience. A probabilistic methodology to assess and evaluate resilience using fragility modelling, probabilistic impact assessment, and adaptation measures was described in [23]. A power system resilience assessment framework for system based on a resilience trapezoid was provided by [25], which used the loss of load frequency and the loss of load expectation to assess resilience. 2) Different from the traditional reliability indices, which are based on load reduction, frequency and duration to measure, various metrics were designed for quantifying resilience. The resilience indices was defined as the ratio of recovery to loss suffered by a system in [26]. Resilience of integrated power and water systems in earthquakes [27] and resilience of complex engineered [28] were developed, using the resilience triangle model proposed by MCEER. Another branch of research [29]–[31] quantified the resilience according to the integral formulas in [32], but the integration interval was different. The above metrics only focused on the performance of system during a disruption, which ignored the characteristics of extreme events. This limited the implementation feasibility when deploying such indices for different extreme events. Currently, there is no universal standard assessment methodology nor metrics for power system resilience assessment. The above research on power system resilience mainly focused on the evaluation of impacts in a specific extreme event. However, the characteristics of different extreme events (e.g., natural disasters, terrorist attacks, etc.) are different from each other.

For assessing typhoon effects on power systems, [33] and [34] introduced probabilistic models to assess the influence of hurricanes, while the modelling of extreme events was based on the HAZUS (a software application provided by FEMA). Different from the methods depending on HAZUS, [35] introduced a method for estimating impacts of typhoon on power transmission lines using a tropical cyclone wind model. A fuzzy clustering-based inference system with a regional weather model was developed to evaluate impacts of hurricanes on power system reliability in [22]. A hurricane

power outage prediction model was proposed by [36], which was based on publicly available data.

On the above premises, this paper proposes a quantitative resilience assessment framework for power transmission systems under typhoon weather, including a new assessment index. Main contributions of this paper include: 1) Unlike relying on existing risk assessment software, the typhoon wind field model for disaster risk assessment is adopted to evaluate impacts of typhoon using publicly available data. 2) A power system restoration model is developed concerning the fault locations, the weather intensity, the repair crew ability, and the emergency response plans. 3) Combining a cell partition method and a sequential Monte Carlo simulation approach, the spatial and temporal impacts of extreme events are assessed, which considers multiple component outages. 4) A new assessment index is proposed, which considers the impact regarding both the duration and intensity of an extreme event. To illustrate the applicability of the proposed framework, the typhoon Vicente's impact on a test system located in the coastal areas of China is studied.

The rest of paper is organized as follows: Section II describes the resilience assessment framework. Section III introduces a wind field model to evaluate the impacts of typhoon on power transmission systems. Section IV develops probabilistic models for resilience assessment. The resilience assessment methodology is presented in Section V. In Section VI, the proposed method is implemented in a numerical case study. Finally, conclusions are given.

## II. FRAMEWORK DESIGN FOR RESILIENCE ASSESSMENT

This section presents a framework for assessing the overall resilience of a power transmission system under an extreme event. The framework in Fig. 1 includes three parts, i.e., an extreme event model, a power system model, and a resilience assessment methodology. This research takes typhoon as an example to illustrate the proposed framework.

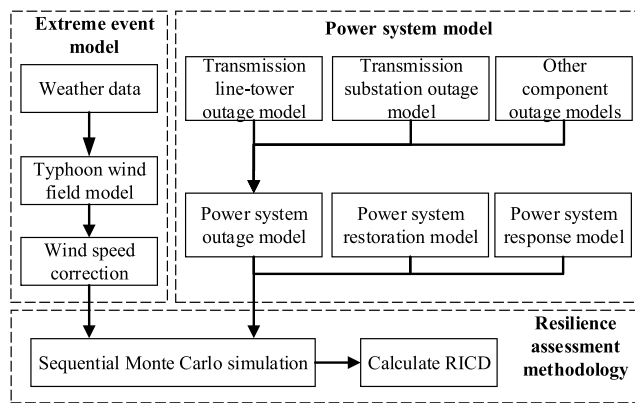


**FIGURE 1.** The resilience assessment framework during extreme events.

1) The first part is the extreme event model, which evaluates impacts using a risk evaluation model for extreme events. The typhoon wind field model for disaster risk assessment is applied to model the intensity and duration of a typhoon.

The mechanism of extreme events affecting power transmission system operation is analyzed based on a cell partition method, which is dividing a system into a number of units.

2) The second is for power system modelling, including a component outage model, a restoration model and a response model. The component outage model expresses the relationship between failure rates of a component of transmission systems and the weather intensity, e.g., wind speed. The restoration model is developed for incarnating restoration processes of power systems, according to specific fault location, weather intensity, repair crew, and the emergency response plans. The behavior of power systems after component failure is described by the response model.

3) The last part is the resilience assessment methodology, which can derive resilience indices based on a sequential Monte Carlo simulation and a cell partition method.

## III. EVALUATION OF TYPHOON IMPACTS

The impacts of typhoon are mainly determined by the intensity and duration of typhoon. This research focuses on the wind impacts on power systems during the period of typhoon, which does not consider derivative disasters.

### A. THE INTENSITY OF IMPACTS

The intensity of impacts can be described by a typhoon wind field model, which is developed to build surface wind fields within a typhoon. If the driving parameters of a typhoon are accurately determined, the wind field within a tropical cyclone can be accurately represented by a parametric wind model [37]. Therefore, considering the simulation accuracy and the computational efficiency, the Yan Meng wind field model is adopted for intensity impact calculation in this research.

#### 1) YAN MENG MODEL

The model is developed for calculating the wind field in a moving typhoon boundary layer considering physical features of a typhoon boundary layer and surface terrain conditions [16]. In this model, the mean sea level pressure  $p$  is computed from (1) proposed by Holland [38].

$$p = p_0 + \Delta p \exp \left( - \left( \frac{R_m}{R} \right)^B \right), \quad (1)$$

where  $B$  set as 0.5~2.5.

The equation of typhoon motion is defined as below [16],

$$\frac{\partial V}{\partial t} + V \cdot \nabla V = - \frac{1}{\rho} \nabla P - f_y \times V + F, \quad (2)$$

where  $\rho$  set at 1.2 kg/m<sup>3</sup>. The typhoon-induced wind velocity  $V$  is calculated as the addition of the gradient wind  $V_g$  in the free atmosphere and the component  $V'$  caused by the friction on the ground surface, i.e.,  $V = V_g + V'$ . Since the frictional force  $F$  is negligible above the boundary layer,

(2) is divided as (3) [16],

$$\begin{cases} \frac{\partial V_g}{\partial t} + V_g \cdot \nabla V_g = -\frac{1}{\rho} \nabla P - fy \times V_g, \\ \frac{\partial V'}{\partial t} + V' \cdot \nabla V' + V' \cdot \nabla V_g + V_g \cdot \nabla V' = -fy \times V' + F. \end{cases} \quad (3)$$

## 2) NUMERICAL SOLUTION

An iterative method is used to gain the roots of the Yan Meng wind field equation (3), and the specific formula simplification is reported in [16]. The gradient wind  $V_g$  is continuously corrected by adding the frictional wind  $V'$ , until the typhoon-induced wind velocity  $V$  converges to a stable value. Finally,  $V$  is derived.

## B. THE DURATION OF IMPACTS

Fig. 2 shows the duration of typhoon impacts on a landing region of a power transmission system. The typhoon centers  $O_a$  and  $O_b$  are the boundary locations of typhoon, which indicate the beginning (i.e.,  $T_0$ ) and end (i.e.,  $T_4$ ) of an typhoon affecting a power transmission system, respectively. The impacted area is considered as inside the radius of the last closed isobar  $R_a$  and  $R_b$ . As a result, the duration of impacts  $t_{dur}$  can be determined as dividing the path of typhoon by the storm moving speed.

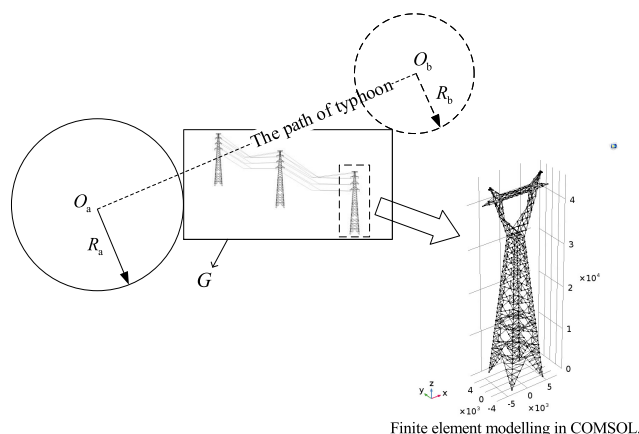


**FIGURE 2.** The duration of typhoon impacts when making landfall on a power transmission system.

## IV. RESILIENCE ASSESSMENT MODEL FOR POWER TRANSMISSION SYSTEMS

In this research, a quantitative resilience assessment framework is proposed for power transmission systems, and the following assumptions are made to reduce the complexity of model, which can still capture key system behaviors.

- The wind speed in a pre-defined cell is consistent within a typhoon wind field.
- Since outdoor components are prone to be affected by a typhoon, in-door substations and generators are considered as 100% reliable during a typhoon.

- All transmission lines utilize the same outage model and all transmission towers also adopt the same type.
- Since the probability of extreme events is small, the data in this respect is limited. Therefore, the repair time, the latitude and longitude of components, component operation data, are produced based on practical experiences in numerical simulation examples.

### A. OUTAGE MODELS FOR TRANSMISSION LINE AND TOWER

Different weather condition severities lead to different failure rates. In this research, a fragility curve [23] is derived to illustrate the relationship between the failure probability and the wind speed, as shown in Fig. 3. Empirical statistical data from utilities can be used to adjust the fragility curve to reflect real behaviors of transmission line and tower.

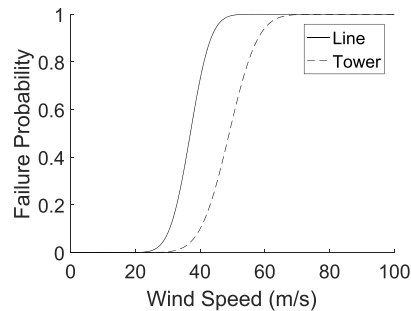


**FIGURE 3.** Fragility curves of transmission line and tower.

### 1) TRANSMISSION LINE OUTAGE MODEL

The breakdown probability of a transmission line segment is given as

$$P_{li} = \Phi(v), \quad (4)$$

where the mean value and the standard deviation are set as 37 and 5, respectively, followed the wind fragility curves in [39].

Considering all the lines in a power transmission corridor as a whole, its failure probability is the convolution of the breakdown probability of each segment, as expressed in (5).

$$\begin{aligned} P_l &= 1 - (1 - P_{l1})(1 - P_{l2}) \cdots (1 - P_{lN_l}) \\ &= 1 - \prod_{i=1}^{N_l} (1 - P_{li}), \end{aligned} \quad (5)$$

### 2) TRANSMISSION TOWER OUTAGE MODEL

During a typhoon, the collapse of transmission tower is mainly caused by the strong wind force of typhoon, which may exceed the design load of a transmission tower. In this research, a finite element method is used to analyze the probability of transmission tower outage at a certain wind speed, which extracts characteristic parameters by simulating the force condition of a transmission tower under a range of wind loadings. The COMSOL Multiphysics software is applied to

analyze the developed structural model, as shown in Fig. 2. The wind load is applied and then the relevant force condition is calculated according to the formulas recommended in Chinese Technical Regulation of Design for Tower and Pole Structure of Overhead Transmission Line (DL/T5154-2002).

The fragility curve of tower under wind load shows the conditional probability that the structural stress or displacement  $S_{s,d}$  exceeds the structural resistance  $R_s$  under different strength levels. Many structural engineering phenomenon have a lognormal distribution. For a given hazard intensity, the breakdown probability of tower  $P_{tj}$  can be described by a lognormal function:

$$P_{tj} = P\left(\frac{R_s}{S_{s,d}} \leq 1\right) = \Phi\left[\frac{-\ln\left(\frac{R_s}{S_{s,d}}\right)}{\beta}\right], \quad (6)$$

For all the towers in a corridor, its failure probability  $P_t$  is the convolution of the breakdown probability of each tower, and the formula structure is the same as (5).

### 3) TRANSMISSION LINE-TOWER OUTAGE MODEL

A line corridor in a transmission network contains multiple transmission towers and lines. In this research, the transmission line-tower outage model for common cause failure is derived based on the distribution of the conditional failure probability of line and tower. Therefore, the breakdown probability of a corridor  $P_c$  is represented as  $P_c = P_l \cup P_t$ .

### B. COMPONENT RESTORATION MODEL

For the conventional reliability assessment for electric power systems, the repair rate of components is generally assumed to be constant. However, the repair rate of a component in a normal weather is different from that under extreme weather events. This research builds a component restoration model by capturing the weather intensity, distance, and restoration resources, which are important in the resilience assessment of power systems. After line or tower outages,  $TTR$  is generated, which represents the time of the whole repair process, and it is composed of the time that the repair crew leave from an office to a site (i.e.,  $TTR_{dis}$ ) and the repair time of components (i.e.,  $TTR_{rep}$ ). In order to develop a component restoration model, three aspects are considered.

- 1)  $TTR$  of component is different between the normal weather and the extreme weather, i.e.,  $TTR_{normal}$  is the repair time of components in the normal weather,  $TTR_{weather}$  is the repair time of components in the non-normal weather. The relationship between  $TTR_{weather}$  and  $TTR_{normal}$  is assumed as (7), where the coefficient  $k_w$  is determined by the weather intensity derived from a wind field model.

$$TTR_{weather} = TTR_{normal} \times k_w. \quad (7)$$

- 2) The repair time of component also includes the time when a team rushes to a fault location, which increases in proportional to the increment of distance between a

departure location of a repair team and a fault location.

$$TTR_{dis} = \frac{s}{v_r} \quad (8)$$

where  $TTR_{dis}$  is the time that a team moves to a fault point.

- 3) All resources are with the same effectiveness to repair. One unit of restoration resources refers to a repair team, and one fault of transmission corridor needs one team to repair it. When the restoration resources are inadequate, the key components should be repaired with priority. Therefore, the repair time of component for waiting  $TTR_{wait}$  needs to be considered.

According to the above principles,  $TTR$  of component is defined as (9).

$$\begin{aligned} TTR_{com} &= TTR_{weather} + TTR_{wait} \\ &= (TTR_{dis} + TTR_{rep}) \times k_w + TTR_{wait}. \end{aligned} \quad (9)$$

### C. POWER SYSTEM RESPONSE MODEL

After a component fails, the state of system is evaluated by its response. In an extreme event, a number of components may be damaged, which separate a power grid into many unconnected sub-grids. Based on the existing models and the characteristics for resilience assessment of a power transmission system under the typhoon weather, the response model in this research is established by following three principles: (a) If there is no power plant in a sub-grid, all the load nodes are assumed as failure; (b) If the sum of all power plant capacities is smaller than the sum of demand, power is rescheduled by cutting the smallest load according to system constraints to balance the total supply and demand. The dispatch command follows calculation results of the DC optimal power flow (OPF); (c) If the sum of all power plant capacities is larger than the sum of demand, power is rescheduled by reducing power generation and the dispatch method is the same as that of (b).

### V. QUANTITATIVE RESILIENCE ASSESSMENT METHODOLOGY

The resilience curve of system status in Fig. 4 shows the trend of system performance following a disruptive event.  $T_0$  is the beginning time of typhoon affecting a transmission system. Before  $T_1$ , the system is in a normal status. From  $T_0$  to  $T_2$ ,

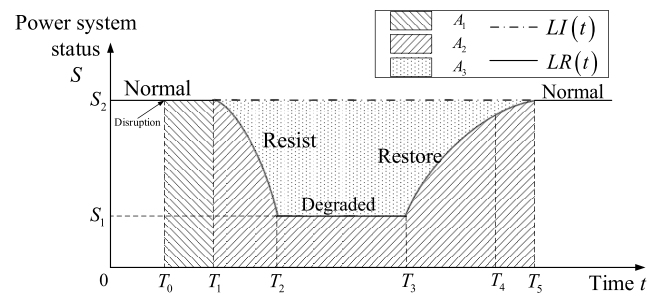


**FIGURE 4.** System status curve of resilience associated with a disruption.

the system resists the disaster and then enters a degraded state from  $T_2$  to  $T_3$ . From  $T_2$  to  $T_5$ , the system responds and restores. The disaster influence on the system finishes at  $T_4$ . The restoration completes and the system returns to the original normal status at  $T_5$ . The solid lines represent the real performance of a power system during an extreme event. The ideal performance of a power system without any deteriorative effects is indicated by the chain-dotted lines.  $A_1, A_2$  and  $A_3$  represent different areas as indicated in Fig. 4. These stages constitute a typical response cycle, which reflect the resistant, absorptive and restorative capacities of a system.

Resilience can be quantified according to the areas between the curve  $LI(t)$  and the curve  $LR(t)$  within the period from  $T_1$  to  $T_5$  [32]:

$$R_t = \int_{T_1}^{T_5} [LI(t) - LR(t)] dt = A_3. \quad (10)$$

Resilience can also be quantified as the ratio of the areas between the curve  $LI(t)$  and the time axis and the curve  $LR(t)$  and the time axis, and the time interval is  $[T_1, T_5]$ , which is also mentioned in [29]:

$$R_r = \frac{\int_{T_1}^{T_5} LR(t) dt}{\int_{T_1}^{T_5} LI(t) dt} / \int_{T_1}^{T_5} LI(t) dt = A_2 / (A_2 + A_3). \quad (11)$$

In this research, a new resilience index (RICD) of a transmission network is proposed, as described in (12).

$$\begin{aligned} R_{RICD} &= E \left[ \frac{\int_{T_0}^{T_5} LR(t) dt}{\int_{T_0}^{T_5} LI(t) dt} \cdot \frac{T_{dur}}{T_5 - T_0} \right] \\ &= \sum_{k=1}^K P_k \left[ \frac{A_1 + A_2}{A_1 + A_2 + A_3} \cdot \frac{T_{dur}}{T_5 - T_0} \right], \end{aligned} \quad (12)$$

where,  $R_{RICD}$  is an expectation.  $T_{dur}$  is the actual duration of typhoon impacts, i.e.,  $T_{dur} = T_4 - T_0$ , as defined in Section III-B.  $P_k$  is calculated based on the Monte Carlo simulation.

RICD is an improvement of (11), which considers the characteristics of an extreme event from the view of the disruption impacts on a target system, i.e., the intensity of impacts and the duration of impacts. It can be applied to compare the resilience for different power systems, as well as in a comparative study to assess the influence of different extreme events. The following improvement is made:

1) The integration interval is defined as  $[T_0, T_5]$ .  $R_t$  and  $R_r$  do not consider the duration of extreme events. Namely, both of them neglect the area  $A_1$ . Most event (e.g., typhoon, ice disaster) impacts are shown as a gradual process, and the system does not degrade at the start of an event if the system is robust enough, i.e., the performance curve degrades at  $T_1$  rather than at  $T_0$ . One of the key features of power system resilience is resistance [11]. Systems with higher resilience are more resistant to maintain the normal operation during  $[T_0, T_1]$ .  $[A_2/(A_2 + A_3)]$  cannot reflect such resistance ability as mentioned before, which neglects the area  $A_1$ , and

it is smaller than  $[(A_1 + A_2)/(A_1 + A_2 + A_3)]$ . Meanwhile,  $\int_{T_0}^{T_5} LR(t) dt / \int_{T_0}^{T_5} LI(t) dt$  is introduced to describe the system degradation, which reflects the intensity of impacts on a target system and is proportional to the system resilience.

2) The duration of impact is considered by introducing  $[T_{dur}/(T_5 - T_0)]$ . As different events are accompanied by different duration of impacts, the resilience cannot be determined only based on the curve of resilience. A system may need a long period to recover (i.e., larger  $(T_5 - T_0)$ ) because weather impacts continue (i.e., larger  $T_{dur}$ ), which does not mean the system is not resilient. If two systems face different disruptions but have the same performance curve during  $T_1$  to  $T_5$ , the system suffering from a disruption with larger  $T_{dur}$  is more resilient. However, neither  $R_t$  nor  $R_r$  considers the effect of  $T_{dur}$ . With the same  $T_{dur}$ , a system is more resilient with a smaller  $(T_5 - T_0)$ , meaning a fast restoration ability between  $T_3$  and  $T_5$ . Therefore, RICD is proportional to  $T_{dur}$ , and the inverse to  $(T_5 - T_0)$ . And  $R_{RICD}$  is also normalized to 1 by introducing  $[T_{dur}/(T_5 - T_0)]$ .

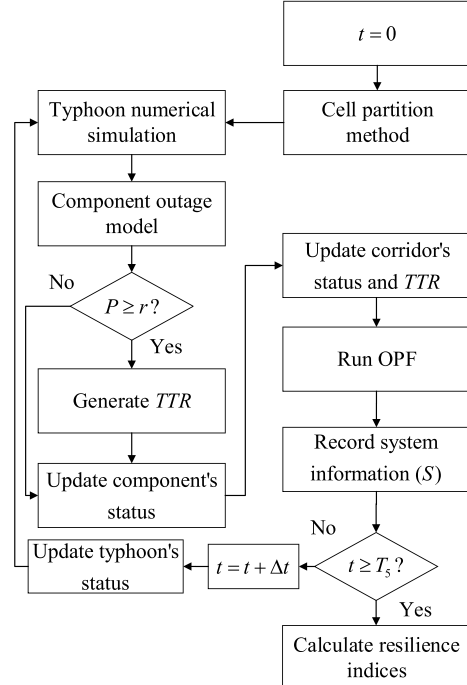


**FIGURE 5.** The proposed procedures for quantitative resilience assessment.

The index calculation procedure corresponding to a probability failure scenario is shown in Fig. 5. The sequential Monte Carlo simulation is applied to calculate the index, and the DC OPF is employed as an appropriate dispatch tool. The system is divided into several cells based on a cell partition method, when the simulation begins. In each step  $\Delta t$ , the state of typhoon is updated, including its location and strength. Based on the location of each component and the corresponding outage model, the failure probability  $P$  is obtained and compared with a random number  $r$  from a uniform distribution, if  $P > r$ , then the component breaks down and  $TTR$  is

generated based on the component restoration model. Consequently, the entire corridor's state and  $TTR$  are obtained, and then run OPF and record system information ( $S$ ). If  $t$  is less than  $T_5$ , the simulation increases a step ( $\Delta t$ ) and continues to run the loop until the termination criterion is reached. If  $t$  equals to  $T_5$ , the simulation terminates.

## VI. NUMERICAL EXAMPLE AND DISCUSSION

In order to verify the effectiveness of the proposed framework, the modified IEEE 6-bus test system assumed to be operated under the typhoon Vicente (which was the eighth tropical storm developed in the Western North Pacific Ocean and the South China Sea in 2012) is studied.

### A. TEST SYSTEM AND DATA

The proposed approach is illustrated using the IEEE 6-bus Reliability Test System (RBTS) [40], as shown in Fig. 6(a). In order to study the spatial impacts of typhoon, each node is assumed to be in the latitude and the longitude as depicted in Table 1 and Fig. 6(b).

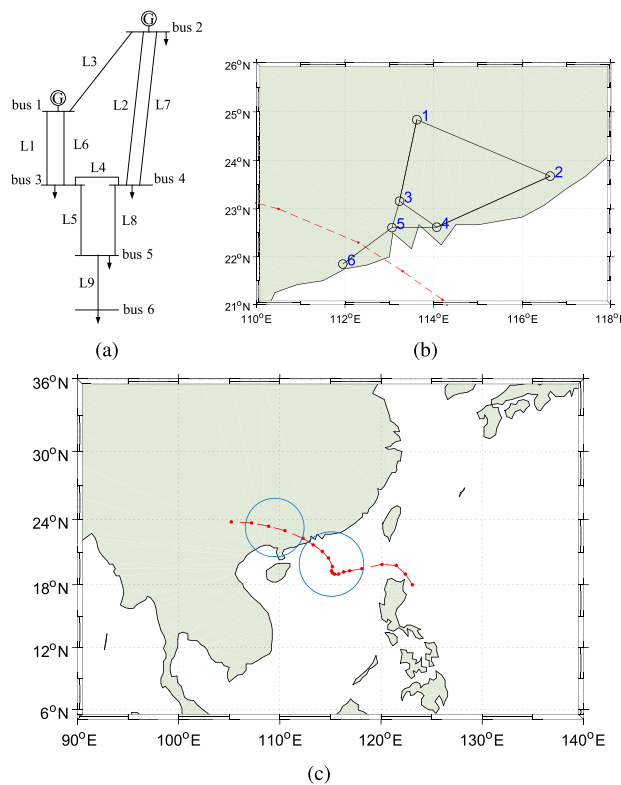


**FIGURE 6.** The test system under the typhoon Vicente. (a) Test system. (b) Geographic diagram of the test system. (c) The path of the typhoon Vicente.

All the data about Vicente, provided by the Joint Typhoon Warning Center (JTWC) [41], are updated every 6 hours in the event of a tropical cyclone. Between the two adjacent warning time, the linear interpolation is used to calculate the time and typhoon's position. The other data (e.g.,  $R_m$  etc.) are set as its maximum to investigate the worst typhoon case. Fig. 6(c) shows the path of the typhoon Vicent as indicated

**TABLE 1.** The location of buses in the test system.

Bus	1	2	3	4	5	6
Longitude( $^{\circ}$ )	113.62	116.63	113.23	114.07	113.06	111.95
Latitude( $^{\circ}$ )	24.84	23.68	23.16	22.62	22.61	21.85

by the dotted line. The solid circle and dotted cirle represent the position of Vicente, at which it begins and stops to influence the test system, respectively. The date of Vicente from 06:00 on July 20, 2012 are used in this investigation.

A structural model of China State Grid cup type tower from [42] is adopted in this example, in which the voltage class is 220 kV and its designing wind speed is 30 m/s. The outage model of transmission lines per 50 km is described by the lognormal function in this numerical example, and the outage model of transmission tower is obtained through the finite element analysis. The fragility curves are shown in Fig. 3. When the restoration resources are insufficient, the corridor priority level is assumed as  $L_3 > L_1 > L_6 > L_2 > L_7 > L_4 > L_5 > L_8 > L_9$ , and it can be adjusted based on the actual situation. The repair crew is assumed to locate at  $(113.06^{\circ}\text{E}, 22.61^{\circ}\text{N})$ .  $TTR_{\text{rep}}$  of a transmission line per 500 meters and a tower are assumed as 1 hours and 5 hours, respectively.  $TTR$  of a power transmission corridor is considered as the sum of  $TTR_{\text{com}}$ . Let  $v_r$  be 60 km/h and  $k_w$  is a random number defined by different damage levels as

$$k_w = \begin{cases} 1 & 0 \leq v \leq 10 \text{ m/s} \\ U(1, 2) & 10 \text{ m/s} < v \leq 20 \text{ m/s} \\ U(2, 3) & 20 \text{ m/s} < v \leq 40 \text{ m/s} \\ U(3, 4) & 40 \text{ m/s} < v \leq 60 \text{ m/s} \\ U(4, 5) & 60 \text{ m/s} < v \end{cases} \quad (13)$$

where  $U$  is a uniform distribution function.

To illustrate the effectiveness of the proposed resilience assessment methodology, four cases are studied.

1) *Case 1 (Base):* It is considered that the restoration resources are abundant, and the outage model and  $TTR$  are the same as discussed in the previous assumptions;

2) *Case 2 (Considering Robustness):* Increasing the designing wind speed of transmission line and tower by 5 m/s compared with *Case 1*;

3) *Case 3 (Considering Shorter Repair Time):*  $TTR_{\text{com}}$  is reduced by a factor of 1/2 compared with *Case 1*;

4) *Case 4 (Considering Restoration Resource Shortage):* Only one team takes part in the repair of system compared with *Case 1*.

In all the cases, the simulation step is set as 15 minutes.

## B. SIMULATION RESULTS AND DISCUSSION

Table 2 lists the results of cell partition in each line, in which each cell represents a segment of 500 meters transmission line divided by a transmission tower. Fig. 7(a) shows the results of each bus during Vicente simulated with the Yang Meng model.

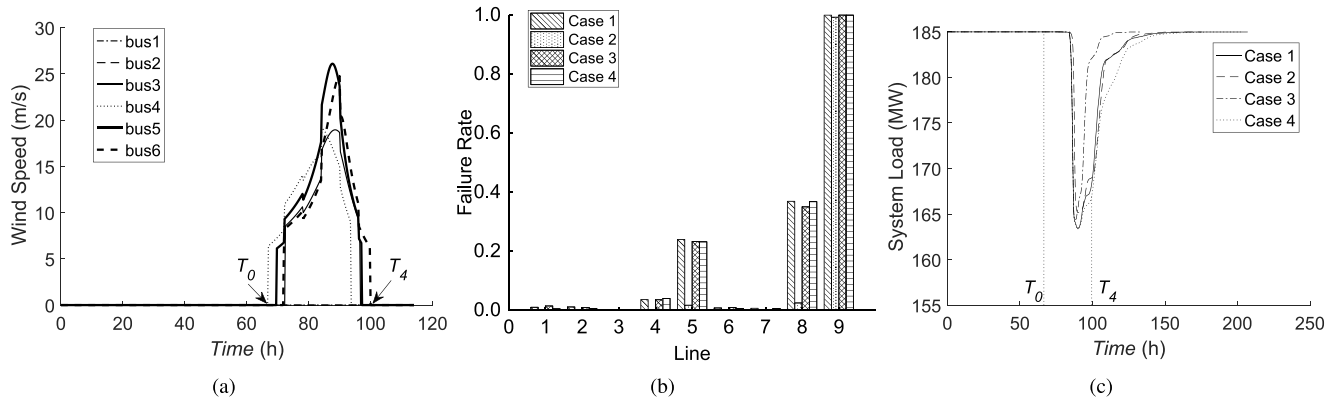


**FIGURE 7.** The simulation results for all cases during typhoon Vicente: a) Wind speeds on each bus; b) Failure rate of each line; c) The system status curve.

**TABLE 2.** The number of segments in each line.

Line	L1, L6	L2, L7	L3	L4	L5	L8	L9
No. of segments	383	575	664	211	128	208	285

It can be clearly seen that wind speeds of bus 1 and bus 2 are 0, as they are far away from the typhoon path. The wind speed decreases with the increase of the distance between the bus and the typhoon path. Since  $R_m$  is maximized and updated every 6 hours, the wind speeds on buses have a sudden change at the moment when  $R_m$  updates. Overall, the curves of each bus have a unimodal distribution, but the size and time of the peak of wind speed are different according to the location of buses with respect to the path of typhoon.

Fig. 7(b) demonstrates the results of failure rate for each line during the typhoon Vicente. The failure rate of L9 for Case 1, Case 3 and Case 4 is 1, and for Case 2 is 0.9916. It can also be seen from Fig. 7(a) and Fig. 7(b) that the failure rate increases obviously with the increase of the wind intensity. For instance, the failure rate of L9 is the highest, as it locates in the region directly crossed by the typhoon. This indicates that the structure strength of L9 needs to be enhanced, so that the operation of L9 is guaranteed during the typhoon.

Comparing Case 1, Case 3 and Case 4 with Case 2, it shows that the failure rate for Case 2 is lower than the other cases for all lines, and their dispersion increases with the increase of the distance between the transmission lines and the typhoon path. In comparison, the difference in failure rates between Case 1, Case 3 and Case 4 is very small.

Fig. 7(c) illustrates the status curves during the typhoon for all the cases, which are represented by the relationship between the system load capacity and the time. As shown in Fig. 7(c), initially the typhoon has little impact on the power transmission system with a low wind speed, and the curves decline after  $T_0$  about 10 hours. Significant differences are observed at the time points, when the status curves decline

and the troughs of curves happen in Case 1 and Case 2. Moreover, the system in Case 3 recovers significantly faster than that in Case 1. At the same time, the system in Case 1 recovers faster than that in Case 4 in the later period of event, when multiple component outage occurs.

**TABLE 3.** The results of resilience indices.

Case	1	2	3	4
$R_{RICD}$	0.8190	0.8206	0.9496	0.7163
$R_t$	388.2702	358.6115	194.0650	472.9654
$R_r$	0.9000	0.9012	0.9308	0.9091

$R_{RICD}$ ,  $R_t$  and  $R_r$  are obtained as listed in Table 3.  $R_{RICD}$  for Case 1 is similar to that of Case 2. The reason for that is the measures, which are the improved designing wind speed by 5 m/s compared with Case 1, are not very effective when facing Vicente. It indicates that component enhancement strategies of power system should be determined according to the predicted path and intensity of disaster, instead of upgrading all components at high cost against an extreme event. Case 3 has the largest  $R_{RICD}$ , which has shorter repair time than the other cases. Additionally, Case 4 considers restoration resource shortage, so its  $R_{RICD}$  is the lowest. It demonstrates that the resources of repair play a critical role in resilience assessment. Comparing  $R_{RICD}$  of Case 3 and Case 4 with Case 1, it is deduced that effective preparedness plans in place, such as improving the repair efficiency, conceiving reasonable emergency strategies and emergency mechanism, are useful measures to boost the grid resilience during extreme events.

Different from  $R_{RICD}$  and  $R_r$ ,  $R_t$  is not normalized to 1 and thus  $R_t$  of different systems are not comparable. As the increase of system resilience, the value of  $R_{RICD}$  increases while the value of  $R_t$  decreases. According to the system configuration of Case 4, the resilience of Case 4 is the weakest among the four cases. However, the system resilience index calculated with  $R_r$  indicates that the resilience of Case 4 is larger than that of Case 1, which violates the actual system configuration. This is due to that  $R_r$  is calculated

by the ratio of  $A_2$  and  $(A_2 + A_3)$  as presented in (11). Owing to the shortage of restoration resource in Case 4, the curve  $LR(t)$  of Case 4 approaches to the curve  $LI(t)$  for a long time in the later period of event. If  $(A_3^1/A_2^1)$  is larger than  $(\Delta A_3^{4-1}/\Delta A_2^{4-1})$  for Case 4,  $A_2/(A_2 + A_3)$  is larger in Case 4 than that in Case 1. The reasoning process of that is shown in (14). Therefore,  $R_r$  fails to indicate the resilience of transmission systems in specific cases, e.g., Case 4. By contrast,  $R_{RICD}$  considers  $[T_{dur}/(T_5 - T_0)]$  as discussed in Section V. The system in Case 4 with a larger  $(T_5 - T_0)$  is less resilient than that in Case 1, and  $R_{RICD}$  of Case 4 is the smallest, which agrees with the actual system configuration. Hence,  $R_{RICD}$  can overcome the limitations of  $R_r$  and  $R_t$ , which is not only normalized to 1, but also can be applied in the assessment considering the system design parameters and the characteristics of disruption.

$$\text{If } \frac{A_3^1}{A_2^1} > \frac{\Delta A_3^{4-1}}{\Delta A_2^{4-1}} \Rightarrow \frac{A_3^1}{A_2^1} > \frac{A_3^4 - A_3^1}{A_2^{4-1}},$$

Rearrange the above equation,

$$A_3^1 A_2^4 - A_3^1 A_2^1 > A_3^4 A_2^1 - A_3^1 A_2^1, \quad (14)$$

Then, cancel  $A_3^1 A_2^1$  and add  $A_2^1 A_2^4$  in both sides, Obtain,

$$\frac{A_2^4}{A_2^4 + A_3^4} > \frac{A_2^1}{A_2^1 + A_3^1},$$

where the superscript represents the number of case,  $\Delta A_2^{4-1}$  and  $\Delta A_3^{4-1}$  are variations of  $A_2$  and  $A_3$  between Case 1 and Case 4, respectively, i.e.,  $\Delta A_2^{4-1} = A_2^4 - A_2^1$ ,  $\Delta A_3^{4-1} = A_3^4 - A_3^1$ . All variables are greater than zero.

## VII. CONCLUSIONS

This paper has developed a quantitative assessment framework to evaluate the resilience of power transmission systems based on a tropical cyclone wind model, which considers the actual path of typhoon. The proposed framework represents an effective way to analyze the resilience of transmission systems considering the weather intensity, fault location of components, restoration resources, and emergency response plans. According to the four case studies of a power transmission system under the typhoon Vicente, RICD is able to reflect the influence of system parameters (i.e., resistance, repair time, restoration resources) and the characteristics of extreme events (i.e., the intensity and duration of disruption) on the resilience. RICD is also able to overcome the limitations of two traditional assessment indices with respect to normalization and comparability. Moreover, the simulation results have highlighted the capability of the proposed methodology in assessing and quantifying the resilience of power transmission systems against typhoons.

## REFERENCES

- [1] W. Li, *Risk Assessment of Power Systems: Models, Methods, and Applications*. Hoboken, NJ, USA: Wiley, 2005.
- [2] L. Guo, C. X. Guo, W. H. Tang, and Q. H. Wu, "Evidence-based approach to power transmission risk assessment with component failure risk analysis," *IET Gener. Transmiss. Distrib.*, vol. 6, no. 7, pp. 665–672, Jul. 2012.
- [3] K. Xie, K. Cao, and D. C. Yu, "Reliability evaluation of electrical distribution networks containing multiple overhead feeders on a same tower," *IEEE Trans. Power Syst.*, vol. 26, no. 4, pp. 2518–2525, Nov. 2011.
- [4] J. Lu, M. Zeng, X. Zeng, Z. Fang, and J. Yuan, "Analysis of ice-covering characteristics of China Hunan power grid," *IEEE Trans. Ind. Appl.*, vol. 51, no. 3, pp. 1997–2002, May 2015.
- [5] N. Mimura, K. Yasuhara, S. Kawagoe, H. Yokoki, and S. Kazama, "Damage from the great east Japan earthquake and tsunami—A quick report," *Mitigation Adaptation Strategies Global Change*, vol. 16, no. 7, pp. 803–818, 2011.
- [6] D. Mendonça and W. A. Wallace, "Impacts of the 2001 world trade center attack on New York city critical infrastructures," *J. Infrastruct. Syst.*, vol. 12, no. 4, pp. 260–270, 2006.
- [7] C. S. Holling, "Resilience and stability of ecological systems," *Annu. Rev. Ecol. Syst.*, vol. 4, no. 1, pp. 1–23, 1973.
- [8] Y. Li and B. J. Lence, "Estimating resilience for water resources systems," *Water Resour. Res.*, vol. 43, no. 7, pp. 256–260, 2007.
- [9] C. W. Zobel and L. Khansa, "Quantifying cyberinfrastructure resilience against multi-event attacks," *Decis. Sci.*, vol. 43, no. 4, pp. 687–710, 2012.
- [10] *Presidential Policy Directive—Critical Infrastructure Security and Resilience*, White House, Washington, DC, USA, 2013.
- [11] *Keeping the Country Running: Natural Hazards and Infrastructure*, Cabinet Office, London, U.K., Oct. 2011.
- [12] A. Aitsi-Selmi, S. Egawa, H. Sasaki, C. Wannous, and V. Murray, "The Sendai framework for disaster risk reduction: Renewing the global commitment to people's resilience, health, and well-being," *Int. J. Disaster Risk Sci.*, vol. 6, no. 2, pp. 164–176, 2015.
- [13] M. Panteli and P. Mancarella, "The grid: Stronger, bigger, smarter?: Presenting a conceptual framework of power system resilience," *IEEE Power Energy Mag.*, vol. 13, no. 3, pp. 58–66, May 2015.
- [14] L. J. Shapiro, "The asymmetric boundary layer flow under a translating hurricane," *J. Atmos. Sci.*, vol. 40, no. 8, pp. 1984–1998, 1983.
- [15] E. F. Thompson and V. J. Cardone, "Practical modeling of hurricane surface wind fields," *J. Waterway, Port, Coastal, Ocean Eng.*, vol. 122, no. 4, pp. 195–205, 1996.
- [16] Y. Meng, M. Matsui, and K. Hibi, "An analytical model for simulation of the wind field in a typhoon boundary layer," *J. Wind Eng. Ind. Aerodynamics*, vol. 56, nos. 2–3, pp. 291–310, 1995.
- [17] I. Dobson, B. A. Carreras, V. E. Lynch, and D. E. Newman, "Complex systems analysis of series of blackouts: Cascading failure, critical points, and self-organization," *Chaos, Interdiscipl. J. Nonlinear Sci.*, vol. 17, no. 2, p. 026103, 2007.
- [18] D. S. Kirschen, D. Jayaweera, D. P. Nedic, and R. N. Allan, "A probabilistic indicator of system stress," *IEEE Trans. Power Syst.*, vol. 19, no. 3, pp. 1650–1657, Aug. 2004.
- [19] L. Dueñas-Osorio and S. M. Vemuru, "Cascading failures in complex infrastructure systems," *Struct. Saf.*, vol. 31, no. 2, pp. 157–167, 2009.
- [20] M. Anghel, K. A. Werley, and A. E. Motter, "Stochastic model for power grid dynamics," in *Proc. 40th Annu. Hawaii Int. Conf. Syst. Sci. (HICSS)*, 2007, p. 113.
- [21] R. Billinton and G. Singh, "Application of adverse and extreme adverse weather: Modelling in transmission and distribution system reliability evaluation," *IEE Proc.-Gener. Transmiss. Distrib.*, vol. 153, no. 1, pp. 115–120, Jan. 2006.
- [22] Y. Liu and C. Singh, "A methodology for evaluation of hurricane impact on composite power system reliability," *IEEE Trans. Power Syst.*, vol. 26, no. 1, pp. 145–152, Feb. 2011.
- [23] M. Panteli, C. Pickering, S. Wilkinson, R. Dawson, and P. Mancarella, "Power system resilience to extreme weather: Fragility modelling, probabilistic impact assessment, and adaptation measures," *IEEE Trans. Power Syst.*, vol. 32, no. 5, pp. 3747–3757, Sep. 2017.
- [24] Z. Bie, Y. Lin, G. Li, and F. Li, "Battling the extreme: A study on the power system resilience," *Proc. IEEE*, vol. 105, no. 7, pp. 1253–1266, Jul. 2017.
- [25] M. Panteli, D. N. Trakas, P. Mancarella, and N. D. Hatzigyriou, "Power systems resilience assessment: Hardening and smart operational enhancement strategies," *Proc. IEEE*, vol. 105, no. 7, pp. 1202–1213, Jul. 2017.
- [26] D. Henry and J. E. Ramirez-Marquez, "Generic metrics and quantitative approaches for system resilience as a function of time," *Rel. Eng. Syst. Saf.*, vol. 99, pp. 114–122, Mar. 2012.
- [27] M. Shinozuka et al., "Resilience of integrated power and water systems," in *Proc. Seismic Eval. Retrofit Lifeline Syst.*, 2003, pp. 65–86.

- [28] F. Ren, T. Zhao, J. Jiao, and Y. Hu, "Resilience optimization for complex engineered systems based on the multi-dimensional resilience concept," *IEEE Access*, vol. 5, pp. 19352–19362, 2017.
- [29] M. Ouyang, L. Dueñas-Osorio, and X. Min, "A three-stage resilience analysis framework for urban infrastructure systems," *Struct. Saf.*, vols. 36–37, no. 2, pp. 23–31, 2012.
- [30] D. A. Reed, K. C. Kapur, and R. D. Christie, "Methodology for assessing the resilience of networked infrastructure," *IEEE Syst. J.*, vol. 3, no. 2, pp. 174–180, Jun. 2009.
- [31] G. P. Cimellaro, A. M. Reinhorn, and M. Bruneau, "Framework for analytical quantification of disaster resilience," *Eng. Struct.*, vol. 32, no. 11, pp. 3639–3649, 2010.
- [32] M. Bruneau and A. Reinhorn, "Exploring the concept of seismic resilience for acute care facilities," *Earthq. Spectra*, vol. 23, no. 1, pp. 41–62, 2007.
- [33] M. Ouyang and L. Dueñas-Osorio, "Multi-dimensional hurricane resilience assessment of electric power systems," *Struct. Saf.*, vol. 48, pp. 15–24, May 2014.
- [34] L. Xu and R. E. Brown, "A hurricane simulation method for Florida utility damage and risk assessment," in *Proc. Power Energy Soc. Gen. Meeting-Convers. Del. Elect. Energy Century*, 2008, pp. 1–7.
- [35] Y. H. Yang, Y. L. Xin, J. J. Zhou, W. H. Tang, and B. Li, "Failure probability estimation of transmission lines during typhoon based on tropical cyclone wind model and component vulnerability model," in *Proc. IEEE PES Asia-Pacific Power Energy Eng. Conf. (APPEEC)*, Nov. 2017, pp. 1–6.
- [36] S. D. Guijema, R. Natafeghi, S. M. Quiring, A. Staid, A. C. Reilly, and M. Gao, "Predicting hurricane power outages to support storm response planning," *IEEE Access*, vol. 2, pp. 1364–1373, 2014.
- [37] A. C. Phadke, C. D. Martino, K. F. Cheung, and S. H. Houston, "Modeling of tropical cyclone winds and waves for emergency management," *Ocean Eng.*, vol. 30, no. 4, pp. 553–578, 2003.
- [38] G. J. Holland, "An analytic model of the wind and pressure profiles in hurricanes," *Monthly Weather Rev.*, vol. 108, no. 8, pp. 1212–1218, 1980.
- [39] M. Panteli, P. Mancarella, D. Trakas, E. Kyriakides, and N. Hatziaargyriou, "Metrics and quantification of operational and infrastructure resilience in power systems," *IEEE Trans. Power Syst.*, vol. 32, no. 6, pp. 4732–4742, Nov. 2017.
- [40] R. Billinton *et al.*, "A reliability test system for educational purposes-basic data," *IEEE Trans. Power Syst.*, vol. 4, no. 3, pp. 1238–1244, Aug. 1989.
- [41] Naval Research Lab, Monterey, and JTWC. *Western North Pacific Ocean Best Track Data*. Accessed: Mar. 25, 2018. [Online]. Available: <http://www.metoc.navy.mil/jtwc/jtwc.html?western-pacific>
- [42] Z. Y. Liu, *Typical Project Design of SGCC Transmission and Substation*. Beijing, China: China Electric Power Press, 2005.



**WENHU TANG** (M'05–SM'13) received the B.Sc. and M.Sc. degrees in electrical engineering from the Huazhong University of Science and Technology, Wuhan, China, in 1996 and 2000, respectively, and the Ph.D. degree in electrical engineering from The University of Liverpool, Liverpool, U.K., in 2004. He was a Post-Doctoral Research Associate and subsequently a Lecturer with The University of Liverpool from 2004 to 2013. He is currently a Distinguished Professor and the Acting Dean of the School of Electric Power Engineering, South China University of Technology, Guangzhou, China. He has authored and co-authored over 100 research papers, including 40 journal papers and one Springer research monograph. His research interests include power systems risk assessment, renewable energy integration in power grids, condition monitoring and fault diagnosis for power apparatus, multiple-criteria evaluation, and intelligent decision support systems. He is a fellow of IET.



**YANG LIU** received the B.Sc. and Ph.D. degrees in electrical engineering from the South China University of Technology (SCUT), Guangzhou, China, in 2012 and 2017, respectively. From 2016 to 2016, he was with The University of Liverpool as an Honorary Associate under the support of the China Scholarship Council. He is currently a Post-Doctoral Researcher in electrical engineering with SCUT. His research interests include the areas of power system control and operation, smart grid resiliency, and renewable energy.



**YANLI XIN** received the B.Sc. degree in electrical engineering from the Jiangxi University of Technology, China, in 2012. She is currently pursuing the Ph.D. degree in electrical engineering with the South China University of Technology, China. Her research interests include electromagnetic transient modeling of power system and resilience modeling of power grid.



**QINGHUA WU** (M'91–SM'97–F'11) received the Ph.D. degree in electrical engineering from The Queen's University of Belfast (QUB), Belfast, U.K., in 1987. He was a Research Fellow and subsequently a Senior Research Fellow with QUB from 1987 to 1991. He joined the Department of Mathematical Sciences, Loughborough University, U.K., in 1991, as a Lecturer; subsequently, he was appointed as a Senior Lecturer. In 1995, he joined The University of Liverpool, Liverpool, U.K., to take up his appointment to the Chair of electrical engineering with the Department of Electrical Engineering and Electronics. He is also with the School of Electric Power Engineering, South China University of Technology, Guangzhou, China, as a Distinguished Professor and the Director of the Energy Research Institute of the University. He has authored and co-authored over 440 technical publications, including 240 journal papers, 20 book chapters, and three research monographs published by Springer. His research interests include nonlinear adaptive control, mathematical morphology, evolutionary computation, power quality, and power system control and operation. He is a fellow of IET and InstMC and a Chartered Engineer.



**YIHAO YANG** received the B.Sc. degree in electrical engineering from Fuzhou University, Fuzhou, China, in 2016. He is currently pursuing the M.Sc. degree with the South China University of Technology, China. His research interests include finite element analysis, power system resilience, and reliability evaluation.